ANALYSIS OF SIX-PORT MEASUREMENT SYSTEMS

Ross A. Speciale
TRW Defense and Space Systems Group
Redondo Beach, California 90278

ABSTRACT

A comparative scattering parameter analysis of various microwave six-port circuit configurations has been performed in relation to applications in single and dual six-port automated microwave measurement systems. The aim of this analysis was a confirmation of the predictions of the existing general six-port theories and a search for possible simplifications of these theories to be achieved through selective restrictions of their generality.

Two circuit configurations have been, so far, analyzed. The first is the proposed preferred configuration having three q-points close to the 120° optimum locations and a fourth q-point at a great distance from the origin. The second is a "pseudo-symmetric" circuit configuration having four q-points nominally at the cardinal points of the Γ-plane unit circle.

Microwave measurement systems based on the six-port principle fully reconstruct complex wave-vector ratios from sets of redundant magnitude-only readings. This leads to determining points in a complex plane as intersections of three or more circles. A simple conformal mapping may be used to visualize the resolution of this method and its sensitivity to errors in the magnitude readings. This mapping transforms families of constant-magnitude-ratio circles in straight parallel lines. The coordinates in the transformed plane are the measured magnitude ratio in dB and the angle between the tangents to the intersecting circles at the intersection points.

INTRODUCTION

Various microwave six-port circuit configurations have been proposed, implemented and used as the basis of alternative forms of automated microwave reflectometers and network analyzers [1 - 4].

Also, a number of very general theories have been developed that describe the performance of any microwave six-port network in this type of application and provide methods for the calibration of automated measurement systems using six-port networks as means for reconstructing the complex ratio of two wave-vectors [5 - 8].

The fundamental characteristic of any microwave six-port network, that determines the performance of the network in these measurement applications is represented by the position of at least four "q-points" in the complex plane of the considered wave-vector ratio (Γ_ℓ or ρ_1 and ρ_2).

Preferred circuit configurations having nominally optimal positions for the q-points have been found and suggested [9].

It appears, however, that no specific effort has been, so far, directed towards correlating specific six-port circuit configurations, implemented with known network elements and the evolution of their q-point positions across the complex plane as a function of frequency. This type of information is, however, highly relevant as it provides a quantitative prediction of the changes in performance of any given six-port configuration in a six-port measurement system across any given frequency band. This information also provides a quantitive basis for mutually comparing different six-port configurations in terms of their measurement performance. The positions of the q-points in the complex plane of the considered vector ratio are linear complex functions of the six-port scattering parameters.

The computation of the entries of the 6 x 6 complex scattering matrix S_{ij} of any given six-port circuit configurations is, thus, the first fundamental step towards performance evaluation.

For any given configuration, the problem is one of scattering network analysis. The problem could be solved analytically through extensive, tedious and costly mathematical developments. It can be solved much faster and with less cost and chance of error by applying one of the existing, proven, general purpose network analysis programs.

SCATTERING PARAMETER ANALYSIS

A comparative scattering parameter analysis of various microwave six-port configurations has been already performed using one large scale, general purpose, interactive network analysis program. This program has the capability of accepting a large variety of network descriptions and of computing and graphically displaying the network's scattering parameters across a given frequency band. Multiport networks may be piece-wise analyzed in terms of reduced 2 x 2 scattering matrices if all the ports but two, selected as input and output, are assumed to be closed upon known terminations.

Two basic six-port circuit configurations have been analyzed. These are represented in Figures 1 and 2. The first (Figure 1) is the well known, preferred six-port configuration proposed by G. F. Engen in [9].

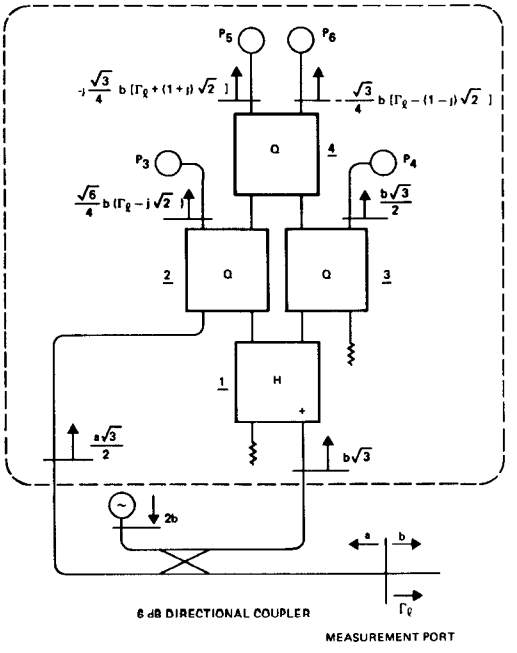

Figure 1. Preferred six-port configuration.

This preferred configuration is implemented with one main directional coupler and four 3 dB hybrids. Three of the hybrids are Q-type or quadrature hybrids. The fourth is an H-type or 180°

hybrid. This configuration has three of the four q-points nominally close to the optimum 120° locations in the complex plane, while the fourth is at infinity.

The second configuration (Figure 2) uses the same components in a slightly different mutual interconnection and it was labelled as the "pseudo-symmetric" six-port. This configuration has all four q-points nominally located on the unit circle and on the four reference semi-axes.

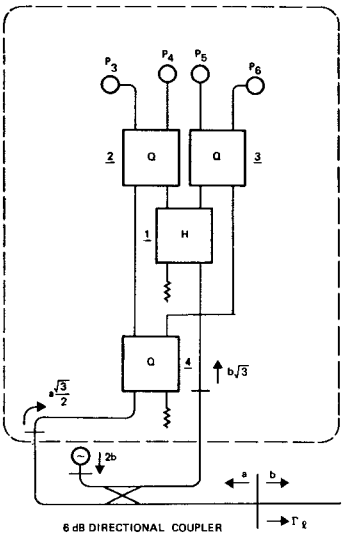

Figure 2. The "Pseudo-Symmetric" six-port configuration.

In the computer analysis of these six-port circuits, the main directional coupler was defined as a 6 dB quarter-wave TEM coupled-line coupler. The Q-type 3 dB hybrids were defined as 3 dB quarter-wave TEM coupled-line couplers. The coupling value could be made nominal at center frequency or at any pair of symmetrically located frequency points on either side of the center frequency. Similarly, the main coupler and the Q-type hybrids could be made fully matched (to a 50 ohm system) or individually mismatched in different amounts and/or having finite rather than infinite directivity, simply by appropriately assigning the even and odd mode impedance values Z_{oe}, Z_{oo} of the two coupled lines. The center frequencies of the main coupler, and of the Q-type hybrids, could also be chosen independently. The H-type hybrid was synthesized as a three-port network consisting of three different, two-port, reciprocal transconductance-elements connected in a Δ between port-pairs (Figure 3). Each two-port, reciprocal transconductance-element is defined by input and output shunt resistances, R_{11} and R_{22}, and by the reciprocal transconductance $G_{12} = G_{21}$.

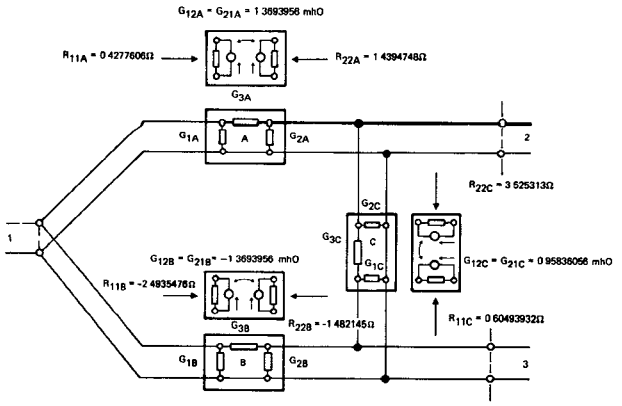

Figure 3. Equivalent circuit of the H-type 3 dB hybrid of Figures 1 and 2 used in the computer analysis of various six-port networks.

The resulting H-type hybrid has 3 dB responses that are independent of frequency.(1)

Twelve different signal paths were analyzed for each given six-port configuration. These signal paths are shown in Figures 4, 5 and 6 as arrows pointing from the port assumed as input to the port assumed as output. All remaining ports, with exception of the measurement port, were assumed to be closed on matched terminations. (All sensors assumed matched.)

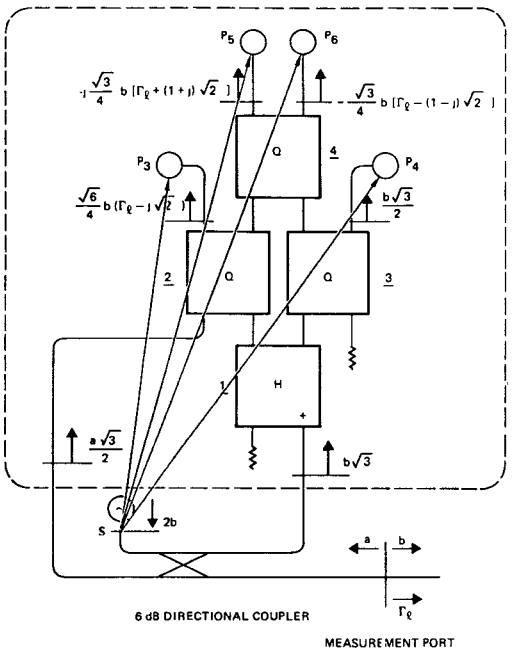

Figure 4. Two-port signal paths used in the scattering analysis of various six-port networks (input at "S").

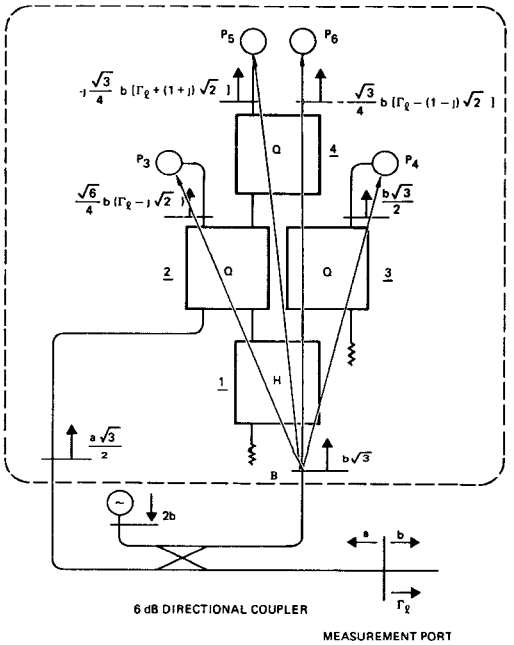

Figure 5. Two-port signal paths used to investigate the response of the microwave correlator to the "b"-wave.

(1)The values in Figure 3 correspond to a 3.1 dB hybrid. The Y-matrix of a 3.0 dB H-type hybrid has infinite entries.

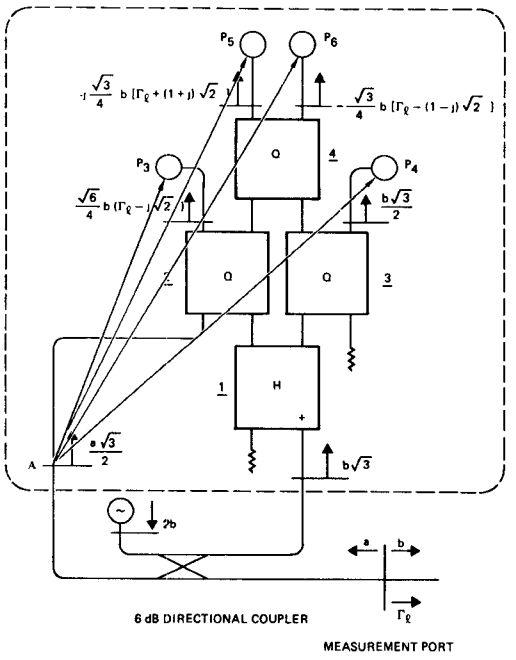

Figure 6. Two-port signal paths used to investigate the response of the microwave correlator to the "a"-wave.

For each path the numerical analysis delivers graphic displays of input and output reflections (S_{11} and S_{22}) in magnitude and phase, as well as the transmission gain and phase ($S_{12} = S_{21}$).

A number of different and typical terminations have been assumed connected to the measurement port in these analyses. These terminations included:

a - A matched load

b - A short

c - An open

d - A 50 ohm line of various lengths, shorted or open at the far end.

e - A very long 50 ohm line terminated by standard reflections ($|\Gamma| = .1, .2, .5$).

In the case e of the long line terminated by standard reflections, the line length and the frequency interval of the analysis were chosen so as to obtain a full 360° rotation of the standard reflection vector at the reflectometer measurement port, while moving the frequency across a negligible fraction of the total bandwidth of the main coupler and of the Q-type 3 dB hybrids. In this way, concentric circles were obtained representing the wave vectors emerging at the four power meter ports. These analyses have so far confirmed all the predictions of the existing six-port theories and demonstrated the ability of the interactive program used to quickly display the effects of any deviation from nominal behavior in the six-port components.

In particular, a sharp frequency evolution of the power meter readings has been predicted in situations where the path length, covered by the reflected signal a, is much longer than the path length covered by the incident signal b. This is a situation that makes the frequency stability of the microwave source used very critical.

The need is thus shown for introducing a compensating delay between the main coupler and the H-type hybrid along the path of the b-wave. This investigation is still in progress, mainly with the aim of searching for possible simplifications of the six-port theory introduced by six-port reciprocity, specific types of symmetry and restriction to almost optimal circuit configurations.

The interactive general purpose network analysis program provides a full scattering parameter description of any given six-port configuration at 200 or more frequencies within a few seconds of CPU time.

The following Figures 7 through 12 present some of the preliminary results obtained during an initial investigation. These results relate to a preferred six-port configuration inplemented with relatively ideal components.

The main 6 dB coupler and the three Q-type hybrids were assumed to be perfectly matched (to 50 ohm), to have infinite directivity, the same center frequency F = 3.0 GHz and to have nominal couplings of 6 dB, respectively 3 dB, at their center frequency.

The plane of the measurement port was assumed coincident with the lower right-hand port of the 6 dB coupler in Figure 1 and all the six-port component were assumed to be directly connected to one another without interconnecting transmission lines.

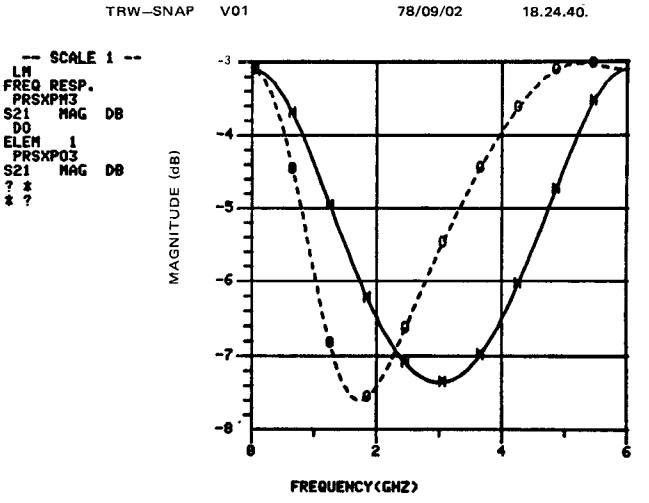

Figure 7. Magnitude response of the signal-path from the source input S to port 3, in the preferred six-port. Solid line marked "M": measurement port matched. Dashed line marked "O": measurement port open. Vertical scale in dB.

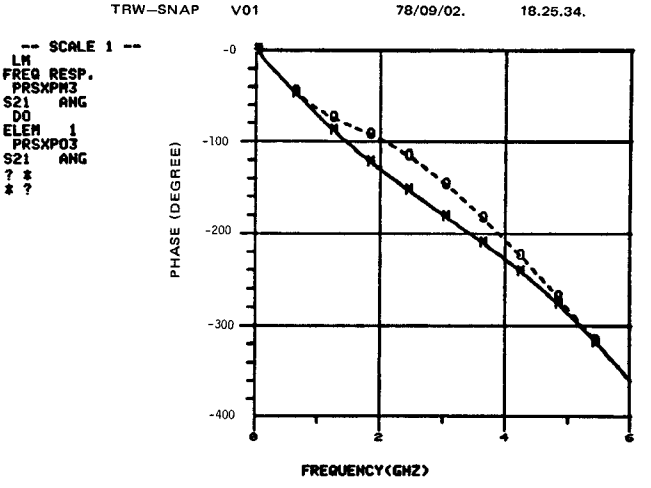

Figure 8. Phase response of the signal path from the source input S to port 3, in the preferred six-port. Solid line marked "M": measurement-port matched. Dashed line marked "O": measurement-port open. Vertical scale in degrees.

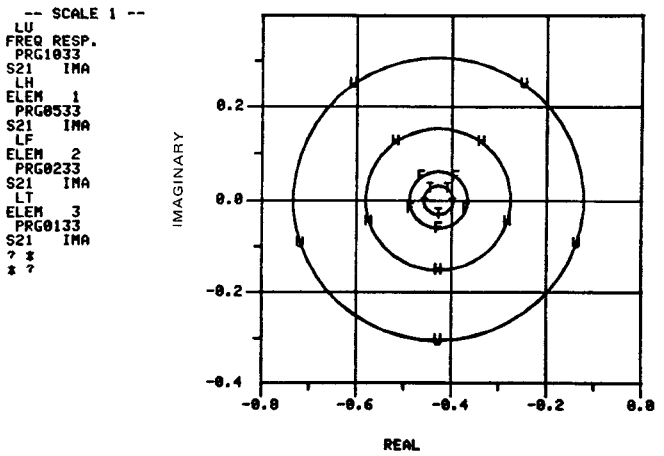

Figure 9. Polar displays of the wave-vector at port 3 of the preferred six-port with a standard reflection evolving through 360° at the measurement-port:
Line marked "U": $|\Gamma|$ = 1.0 (unit)
Line marked "H": $|\Gamma|$ = 0.5 (half)
Line marked "F": $|\Gamma|$ = 0.2 (fifth)
Line marked "T": $|\Gamma|$ = 0.1 (tenth)
F = 3.0 GHz (center frequency for Q-type hybrids).

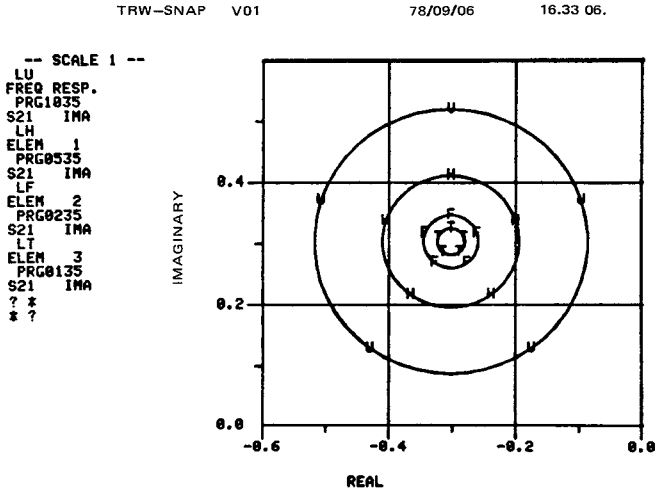

Figure 10. Polar display of the wave-vector at port 6 of the preferred six-port with a standard reflection evolving through 360° at the measurement port:
Line marked "U" $|\Gamma|$ = 1.0 (unit)
Line marked "H": $|\Gamma|$ = 0.5 (half)
Line marked "F": $|\Gamma|$ = 0.2 (fifth)
Line marked "T": $|\Gamma|$ = 0.1 (tenth).

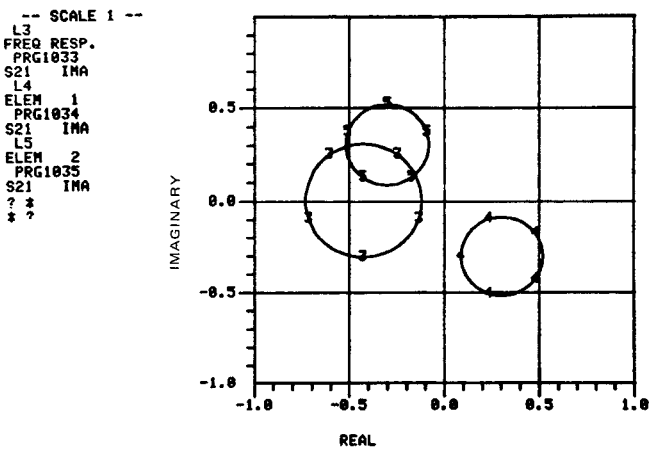

Figure 11. Polar displays of the wave-vector at ports 3, 5 and 6 of the preferred six-port with a total reflection ($|\Gamma|$ = 1.0) evolving through 360° at the measurement port:
Line marked "3": Port 3
Line marked "4": Port 5 See Figure 1
Line marked "5": Port 6
F = 3.0 GHz (center frequence for Q-type hybrids).

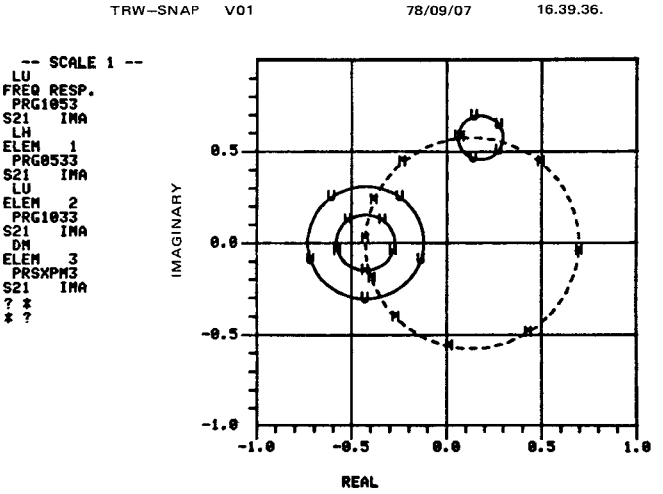

Figure 12. Polar display of the wave-vector at port 3 of the preferred six-port with standard reflections evolving through 360° at the measurement port. Circles at left correspond to F = 3.0 GHz. Dashed circle marked "M" corresponds to a matched termination with F from 25 MHz to 6 GHz. Circle on Top $|\Gamma|$ = 1.0, F = 5.0 GHz.

ANALYSIS BY CONFORMAL MAPPING

The application of microwave six-port networks to measurement systems for the determination of complex wave-vector ratios from magnitude-only readings is widely documents [1 - 6].

In the fundamental case of a single-six-port microwave reflectometer, complex reflection coefficient values, represented by points in the complex Γ plane, are reconstructed from sets of redundant magnitude-only readings. The representing points of the reconstructed complex Γ-values are determined as intersections of at least three circles drawn in the Γ-plane.

The centers of these intersecting circles are the positions of the "q-points" of the specific six-port used, corresponding to the given measurement frequency. These points may be defined as representing the complex Γ-values that force the various magnitude (or power) readings one-by-one to zero, when presented at the reflectometer measurement port.

Any calibration procedure for single-six-port reflectometers must, at least implicitly, reconstruct the positions of these q-points at any given measurement frequency. This reconstruction starts from multiple sets of magnitude-only readings, acquired through calibration measurements, with special standards connected at the measurement port.

The determination of calibrated complex Γ-values for unknown microwave one-port networks uses the reconstructed q-point positions and additional magnitude (or power) readings to determine the multiple circle intersections in the complex Γ-plane.

All the magnitude (or power) readings involved in these processes are, however, affected by finite resolution and random noise. The resolution is essentially determined by the system digitizer used. The system's noise originates partly in the microwave signal source, in the magnitude (or power) sensors and in the digitizer itself.

This leads to a finite uncertainty in the determination of the q-point positions and of the lengths of the radii of the various intersecting circles. The analytical relationship between these uncertainties and the final residual uncertainty of the reconstructed, calibrated Γ-value measurement, in terms of magnitude error and phase error, is not obvious.

A simple conformal mapping transformation may, however, be used to visualize this relationship in graphic display form.

It is known from [10] that the locus of the possible Γ-values corresponding to a constant magnitude ratio (Figure 13):

$$\frac{|\Gamma - q_j|}{|\Gamma - q_i|}$$

is a circle with center on the straight line through q_i and q_j. If then this magnitude ratio is permitted to take different values, a family of circles is generated that resembles the cross-sections of the surfaces of constant potential associated with a parallel-wire transmission line, having the wire-centers on the points q_i and q_j.

It is also known that this particular pattern of constant-potential lines in a bidimensional electrostatic field is amenable to much simpler description by using an appropriate conformal mapping transformation [11].

In Figure 14, an unknown complex reflection coefficient value $\Gamma_x = |\Gamma_x| e^{j\gamma_x}$, represented in the complex $\Gamma = \Gamma_R + j\,\Gamma_I$ plane, is transformed through a change of coordinate system. The new pair of reference axes $\Gamma' = \Gamma'_R + j\,\Gamma'_I = |\Gamma'| e^{j\gamma'}$ has the real axis Γ'_R through the given points q_i and q_j and the origin 0' on the median point between q_i and q_j. This transformation may be expressed in complex form as:

$$\Gamma'_x = e^{-j\alpha}(\Gamma_x - R) = A \cdot \Gamma_x + B \tag{1}$$

where:

$$R = \frac{1}{2}\,(q_i + q_j) \tag{2}$$

$$e^{j\alpha} = \sqrt{\frac{q_j - q_i}{q_j^* - q_i^*}} = A \tag{3}$$

$$B = -\,e^{-j\alpha} \cdot R = -A \cdot R \tag{4}$$

q_j^* and q_i^* being the complex-conjugates of q_j and q_i.

In this new coordinate system the points q_j and q_i map into the real Γ' values:

$$q_j' = \frac{e^{-j\alpha}}{2}\,(q_j - q_i) = q \tag{5}$$

and

$$q_i' = -\,\frac{e^{-j\alpha}}{2}\,(q_j - q_i) = -q \tag{6}$$

In the new complex plane $\Gamma' = \Gamma'_R + j\,\Gamma'_I$ the locus of the Γ' points corresponding to a constant magnitude ratio:

$$\rho = \frac{|\Gamma' - q_j'|}{|\Gamma' - q_i'|} = \frac{|\Gamma' - q|}{|\Gamma' + q|} \tag{7}$$

is a circle with center at:

$$\Gamma' = \lambda = q\,\frac{1 + \rho^2}{1 - \rho^2} \tag{8}$$

and radius

$$r = q\,\frac{2\rho}{|1 - \rho^2|} \tag{9}$$

For different values of the magnitude ratio ρ a family of such circles is generated. These circles map to parallel vertical lines in a plane w, defined by:

$$w = 20 \log_{10}(e) \ln\left(\frac{\Gamma'_x - q}{\Gamma'_x + q}\right) =$$

$$20 \log_{10}(e) \ln\left(\frac{|\Gamma'_x - q|}{|\Gamma'_x + q|}\right) + j\,20 \log_{10}(e) \cdot \underline{\left/\frac{\Gamma'_x - q}{\Gamma'_x + q}\right.} = u + j\,v \tag{10}$$

In the complex w-plane the real coordinate u is expressed by:

$$u = 20 \log_{10}(e) \ln\left(\frac{|\Gamma'_x - q|}{|\Gamma'_x + q|}\right) = 10 \log_{10}(e) \cdot \ln\left(\frac{1 + x^2 - 2x \cos\gamma'_x}{1 + x^2 + 2x \cos\gamma'_x}\right) \tag{11}$$

where

$$x = \frac{|\Gamma'_x|}{q} \tag{12}$$

and

$$\gamma'_x = \arg(\Gamma'_x) \tag{13}$$

and it expresses the ratio of the signal magnitudes measured at ports j and i

$$u = 20 \log_{10}\left(\frac{|\Gamma_x - q_j|}{|\Gamma_x - q_i|}\right) \tag{14}$$

in dB.

Also, in the same complex w-plane the imaginary coordinate v is expressed by:

$$v = 20 \log_{10}(e) \arg\left(\frac{\Gamma'_x - q}{\Gamma'_x + q}\right) = 20 \log_{10}(e) \arctan\left(\frac{2 \sin\gamma'_x}{x - \frac{1}{x}}\right) \tag{15}$$

and it is proportional to the angle between the tangents to the intersecting circles, with centers in q_i and q_j, that determine the position of the point representing Γ_x in the $\Gamma = \Gamma_R + j\,\Gamma_I$ plane.

The information conveyed by u and v is clearly related to resolution and accuracy. The magnitude ratio u is the physical quantity acquired through magnitude (or power) measurements at ports i and j and, as such, is affected by finite resolution and errors. These are functions of the value of u in dB. At the same time circles centered in q_i and q_j have well-defined intersections only if the angle $arg\,[(\Gamma_x - q_j)/(\Gamma_x - q_i)]$ is close to $\pm\frac{\pi}{2}$.

Also, by substituting the coordinate transformation 1) in 10) a single conformal mapping of Γ_x-to-w may be obtained:

$$w = 20 \log_{10}(e) \ln\left(\frac{\Gamma_x - q_j}{\Gamma_x - q_i}\right) \qquad (16)$$

where the complex values q_i and q_j act as transformation parameters. This means that for n q-points there are $\frac{1}{2}$ n (n - 1) possible Γ_x-to-w conformal mapping transformations as given by 16). In a six-port n = 4 so that we have a total of 6 possible transformations, each related to a different pair of q-points.

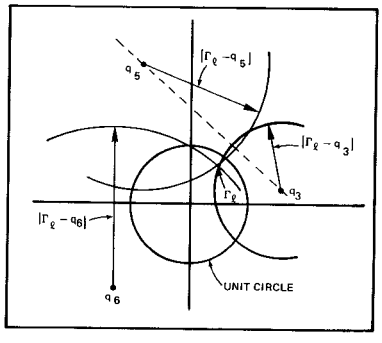

Figure 13. The determination of a Γ_ℓ value from magnitude - only measurements leads to finding the intersection of three or more circles drawn in the complex plane.

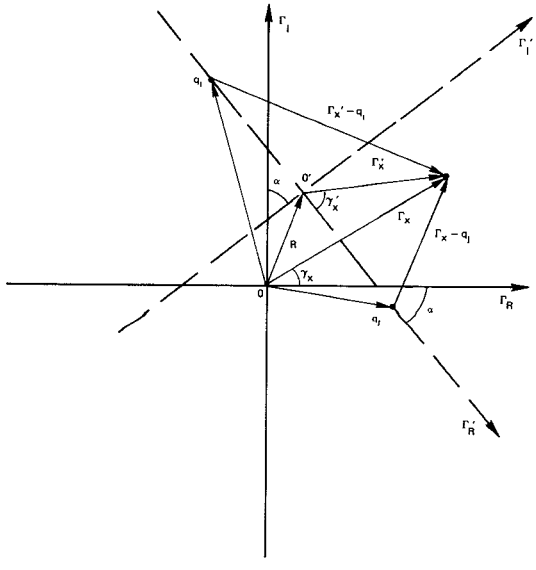

Figure 14. Coordinate transformation of a complex reflection coefficient value Γ_x to reference axes determined by the q-point pair $(q_i - q_j)$.

By mapping standard polar or cartesian grids, drawn in the $\Gamma = \Gamma_R + j\,\Gamma_I$ plane to all 6 these w-planes the uncertainties introduced by the finite magnitude-ratio errors Δu may be visualized, for each pair of q-points, in terms of magnitude error $\Delta|\Gamma|$ or phase error $\Delta\gamma$. These errors may be relatively large for one pair of q-points, and smaller for another. The contribution of the various q-point pairs to the final uncertainty of the Γ value may then be determined.

The paper will present and discuss various computer-generated mappings of standard Γ-plane grids, correlating the resolution of the reconstructed Γ-value to the position of the q-points for various degree of resolution in the determination of the magnitude (or power) ratios.

REFERENCES

1. Hoer, C. A., "Using Six-Port and Eight-Port Junctions to Measure Active and Passive Circuit Parameters," National Bureau of Standards Technical Note No. 673, September 1975.

2. Hoer, C. A., "Calibrating Two 6-Port Reflectometers with Only One Impedance Standard," National Bureau of Standards Technical Note No. 1004, June 1978.

3. Weidman, M. P., "A SemiAutomated Six-Port for Measuring Millimeter - Wave Power and Complex Reflection Coefficient," IEEE Trans. on Microwave Theory and Techniques, Volume MTT-25, No. 12, pp. 1083-1085, December 1977.

4. Hoer, C. A., "A Network Analyzer Incorporating Two Six-Port Reflectometers," IEEE Trans. on Microwave Theory and Techniques, Volume MTT-25, No. 12, pp. 1070-1074, December 1977.

5. Engen, G. F., "Calibration of an Arbitrary Six-Port Junction for Measurement of Active and Passive Circuit Parameters," IEEE Trans. on Instrumentation and Measurements, Vol. IM-22, No. 12, pp. 295-299, December 1973.

6. Engen, G. F., "Calibrating the Six-Port Reflectometer," IEEE MTT-S 1978 International Microwave Symposium, Ottawa, Canada, Digest of Technical Papers, IEEE Catalog No. 78 CHI355 - MTT, pp. 182-183.

7. Engen, G. F., "An Improved Method for Calibrating the Six-Port Reflectometer," National Bureau of Standard Technical Note, 1978.

8. Hoer, C. A., "Using an Arbitrary Six-Port Junction to Measure Complex Voltage Ratios," IEEE Trans. on Microwave Theory and Techniques, Vol. MTT-23, No. 12, pp. 978-984, December 1975.

9. Engen, G. F., "An Improved Circuit for Implementing the Six-Port Technique of Microwave Measurements," IEEE Trans. on Microwave Theory and Techniques, Vol. MTT-25, No. 12, pp. 1080-1083, December 1977.

10. Engen, G. F., "The Six-Port Reflectometer: An Alternative Network Analyzer," IEEE Trans. on Microwave Theory and Techniques, Vol. MTT-25, No. 12, pp. 1075-1080, December 1977. (See in Particular p. 1078, Col 1)

11. Pipes, L. A., "Applied Mathematics for Engineers and Physicists," McGraw-Hill, 1958, Second Edition, pp. 561-565.